

NUMERICAL STUDY OF THE INJECTION CONDITIONS EFFECT ON THE BEHAVIOR OF HYDROGEN-AIR DIFFUSION FLAME

by

**Mohamed BOUKHELEF^a, Mounir ALLICHE^{b*},
Mohammed SENOUCI^{a,c}, and Habib MEROUANE^a**

^aLaboratory of Physic Quantic and Mathematical Modelization of Matter (LPQ3M),
University of Mascara, Mascara, Algeria

^bRenewable Energy and Materials Laboratory (LERM), Faculty of Technology,
University of Medea, Medea, Algeria

^cHigher School in Electrical and Energy Engineering of Oran, USTO, Oran, Algeria

Original scientific paper

<https://doi.org/10.2298/TSCI210530314B>

In order to respond to the increased demand for clean energy without harming the atmosphere through polluting emissions, energy production from the hydrogen combustion become largely used. This work presents a numerical study of the injection conditions effect on the structure of the H₂-air diffusion flame. The aim is to reproduce a practical case of non-polluting combustion and resulting in very high temperatures. The configuration is composed of two axisymmetric coaxial jets, as can be found in the diffusion burners. A presumed probability density function approach is used to describe the chemistry-turbulence interaction. The k-ε model of turbulence is used. Particular attention is given to phenomena anchoring or blowout of the flame.

Key words: *diffusion flame, H₂-air, PDF, turbulence, k-ε model, CFD*

Introduction

The development of energy systems requires substantial support in terms of fossil resources. The activities inherent to domestic and industrial needs require the supply of fuels, the majority of which are hydrocarbons. In addition availability and cost issues, products derived from petroleum and natural gas provide great energy, but release large amounts of pollutants [1, 2]. As a result, the international community is turning to alternative fuels, offering good ecological performance at attractive production costs [3-6].

In this context, hydrogen appears to satisfy these criteria. In fact, it offers a low energy level at ignition and has a wide range of flammability, but still has the disadvantage of having a low density and to be very diffuse, which leads to technological problems, respectively related to sealing and storage [7, 8]. Although premixed flames are less polluting and more used in energy installations as diffusion flames, premixed hydrogen-air flame presents great risks of transition detonation and return of flames (flashback) [9-11].

As a fuel, hydrogen is involved in a several applications from internal combustion engines where it is mixed with natural gas, through gas turbines (mixed with methane) to (H₂-air) burners (low NO_x), and rocket engines (H₂-O₂) [12-15].

* Corresponding author, e-mails: alliche.mounir@univ-medea.dz; alliche_m@yahoo.fr

The aim of this investigation is to use CFD approach as an effective computer based simulation to study and develop the hydrogen combustion processes [16]. Several constraints can get involved to make an experiments of combustion not recommended where, these ones may cause a harmful danger to the entourage [2, 5]. For the hydrogen combustion case is even worse, due to the characteristics of the hydrogen substance itself. This is the reason why it is preferred to use a high fidelity computation systems [16-18]. The CFD and modelling techniques are becoming increasingly important tools to assess the impact of hydrogen combustion in the operating burners [2, 15]. Developments in the field of computer simulation would be extremely useful in predicting flames and combustion process, without the need for expensive and time-consuming field tests. However, the complete description of particle trajectories, chemistry reactions and energy production is needed. This numerical investigation is about making a numerical approach to comprehend how injection conditions can affect the hydrogen flame behavior which is dependent to the same geometric configuration [5, 16].

In the present study, the impacts of tube diameter and fuel velocity on combustion efficiency were examined. The present work mainly concerns the numerical simulation of the phenomenon of turbulent combustion, in a non-premixed flame of the H₂-air type. The aim is to produce a numerical investigation of non-polluting combustion and giving rise to very high temperatures (of the order of 2000 K) [19]. The studied configuration is composed of two co-axial axis-symmetric jets, such as can be found in diffusion burners. In this simulation, the *k-ε* turbulence model was used with a reduced chemical mechanism. We examine the effect of injection conditions on the structure of the diffusion flame, more specifically, speed, temperature and static pressure. We are particularly interested in the phenomena of attachment or blowing of the flame.

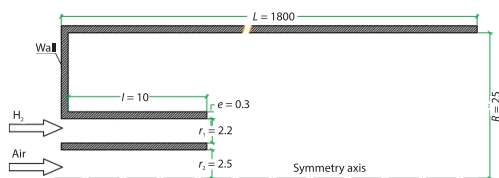


Figure 1. Geometrical configuration

N₂% = 78.992%) is sent via the axial injector at a temperature $T_{air} = 300$ K, with a turbulence intensity of the order of 15% which corresponds to a fluctuating speed given:

$$V'_{air} = \frac{15}{100} \bar{V} \quad (1)$$

The combustible stream (H₂% = 100%) is blown peripherally by the annular injector with an average speed $V_{H_2} = 200$ m/s and a temperature $T_{H_2} = 300$ K. The blowing is characterized by an intensity of turbulence equal to 15%:

The injection Reynolds number related to the fuel flow is given:

$$\Re_{H_2} = \frac{\rho_{H_2} \bar{V}_{H_2}}{\mu_{H_2}} r_1 = 8934 \quad (2)$$

Mathematical modelling

In this study, a CFD approach is applied. The prediction of the aerothermochemical variables of fluid-flow is available by solving the RANS equations, energy and transport of

Operating conditions

The studied configuration is a set of two turbulent jets in an axis-symmetric burner, composed of a coaxial injector, (r_1 and r_2 , of length, l , opening on a cylindrical pipe of length, L , and radius, R , fig. 1. An air stream of standard composition (O₂% = 21.008%,

chemical species [20-22]. Turbulence is described by $k-\varepsilon$ model [16-25]. This is useful in order to correct an overestimation due to radial expansion of the round jet coming from the ring injector [26, 27].

Thus, the governing equations include the continuity eq. (3), momentum eq. (4), and additional conservation equations, such as energy eq. (6) and species concentrations eq. (7). In turbulence circumstance, two others equations are added eqs. (10) and (11).

We can write these equations as following [20-28]:

– Continuity equation

$$\frac{\partial \rho}{\partial t} + \frac{\partial}{\partial x_i}(\rho u_i) = 0 \quad (3)$$

– Momentum equations

$$\frac{\partial}{\partial t}(\rho u_i) + \frac{\partial}{\partial x_i}(\rho u_i u_j) = -\frac{\partial p}{\partial x_i} + \frac{\partial}{\partial x_j} \left[\mu \left(\frac{\partial u_i}{\partial x_j} + \frac{\partial u_j}{\partial x_i} - \frac{2}{3} \delta_{ij} \frac{\partial u_l}{\partial x_l} \right) \right] + \frac{\partial}{\partial x_j}(-\rho \overline{u_i' u_j'}) \quad (4)$$

For combustion cases, all fluids are assumed as Newtonian and the viscous stress tensor:

$$\tau_{ij} = \mu \left\{ \frac{\partial u_i}{\partial x_j} + \frac{\partial u_j}{\partial x_i} \right\} - \frac{2}{3} \mu \delta_{ij} \left\{ \frac{\partial u_k}{\partial x_k} \right\} \quad (5)$$

where μ is the molecular viscosity which depends on the fluid. The Kronecker delta is $\delta = 1$, if $i = j$, 0 otherwise.

– Energy equation

$$\frac{\partial}{\partial t}(\rho E) + \nabla \cdot [\vec{V}(\rho E + p)] = \nabla \cdot \left[k_{\text{eff}} \nabla T - \sum_j h_j \vec{J}_j + (\tau_{\text{eff}} \vec{V}) \right] + S_h \quad (6)$$

where k_{eff} is the effective conductivity, J_j – the diffusion flux of species j , and S_h – the combination of heat chemical reactant and every other heat resource which are defined.

– Species equation

$$\frac{\partial(\rho Y_\alpha)}{\partial t} + \frac{\partial(\rho u_j Y_\alpha)}{\partial x_j} = -\frac{\partial J_j^\alpha}{\partial x_j} + w_\alpha, \quad \alpha = 1, 2, 3, \dots, n \quad (7)$$

where n is the number of species, J_j^α – the molecular diffusivity flux of the species α in the j^{th} co-ordinate direction, w_α – the mass reaction rate of this species per unit volume, and Y_α – the mass fraction of species α .

The diffusive flux, J_j^α , can be approximated:

$$J_j^\alpha = -\frac{\mu}{\text{Sc}_\alpha} \frac{\partial Y_\alpha}{\partial x_j} = -\rho D_\alpha \frac{\partial Y_\alpha}{\partial x_j} \quad (8)$$

where Sc_α is the Schmidt number of the species α , defined:

$$\text{Sc}_\alpha = \frac{\mu}{\rho D_\alpha} \quad (9)$$

where D is the molecular diffusivity of the species α relative to the other species.

Turbulence-combustion modelling

The RANS are used to calculate the transport of the averaged flow quantities, with the entire range of turbulent time and length scales being modeled. The RANS approach greatly reduces the required computational effort and resources compared to LES and DNS. This is why RANS method is widely adopted for practical engineering applications.

In this work, the RNG k - ε turbulence model is used for determining the turbulence behavior which defined by the transport equations [5, 28, 29]:

$$\frac{\partial}{\partial t}(\rho k) + \frac{\partial}{\partial x_i}(\rho k u_i) = \frac{\partial}{\partial x_j} \left[\alpha_k \mu_{\text{eff}} \frac{\partial k}{\partial x_j} \right] + G_k + G_b - \rho \varepsilon - Y_M + S_k \quad (10)$$

$$\frac{\partial}{\partial t}(\rho \varepsilon) + \frac{\partial}{\partial x_i}(\rho \varepsilon u_i) = \frac{\partial}{\partial x_j} \left[\alpha_\varepsilon \mu_{\text{eff}} \frac{\partial \varepsilon}{\partial x_j} \right] + C_{1\varepsilon} \frac{\varepsilon}{k} (G_k + C_{3\varepsilon} G_b) + C_{2\varepsilon} \frac{\varepsilon^2}{k} - R_\varepsilon + S_\varepsilon \quad (11)$$

$$\mu_t = \rho C_\mu \frac{k^2}{\varepsilon} = C_\mu \rho \vartheta \varrho \quad (12)$$

$$R_\varepsilon = \frac{C_\mu \rho \eta^3 (1 - \eta \eta_0) \varepsilon^2}{1 + \beta \eta^3 k} \quad (13)$$

where ϑ the velocity is scale and ϱ – the length scale [30].

All the coefficients of eqs. (10)-(13) are illustrated in tab. 1.

Table 1. Constants values used for turbulence models [29]

	C_μ	σ_k	σ_ε	$C_{1\varepsilon}$	$C_{2\varepsilon}$
RNG k - ε	0.0845	1.3900	1.3900	1.4200	1.6800

where $\eta \equiv Sk\varepsilon$, $\eta_0 = 4.38$, and $\beta = 0.012$, [29].

The effective viscosity is given by the next equation:

$$\mu_{\text{eff}} = \mu + \mu_t \quad (14)$$

where μ is the eddy-viscosity and μ_t – the turbulence viscosity.

The hydrogen combustion phenomena is modeled by using PDF/equilibrium mixture fraction technic [18, 22, 30]. The PDF combustion model is based on the mixture fraction approach with an assumption of fast chemistry [4, 16]. This, offers some advantages over the EDS or EDS-finite-rate models. In addition, it allows intermediate species prediction, more thorough turbulence-chemistry coupling [6, 15, 30].

In order to determine how the injection conditions influenced the hydrogen flame behavior, this study is divided in two parts; in the first, one air (23% O₂, 79% N₂) is used as oxidizer; the chemical kinetics reactions used is reduced mechanism of twelve steps reactions and nine species. The second one pure O₂ (100% O₂, 0% N₂) with twelve steps reactions and eight species. The two cases are based on Boivin's mechanism [31].

To solve the RANS equation, a turbulence model is used for determining the turbulence behavior in the momentum equations and, a combustion model is used to obtain the time-averaged reaction rate for the both energy and space continuity.

In this work, the turbulence is modeled using the RNG k - ε turbulence model. The hydrogen combination is treated using the PDF-equilibrium mixture fraction model. Also, the heat transfer is treated via the discrete-beam method [22, 30].

Numerical method

In this investigation, we have used the CFD package Ansys FLUENT 12.0 in order to model combustion and heat transfer phenomenon in a diffusion hydrogen-air (or hydrogen-di-oxygen) flame. All the governing equations including momentum, energy, species transport, turbulence and chemical reactions are solved using the finite volume approach coupled to turbulence and PDF models. The velocity and pressure fields are linked via SIMPLEC algorithm. The grid nodes are interpolated via the second-order schemes [22].

The numerical simulations are carried out on 2-D, axis-symmetric, quadrilateral and non-uniform grid-mesh of co-ordinates 14442 cells. The grid spacing decreases far from the reaction zones, the mesh form is illustrated on fig. 2. A grid independence test was performed which it leads to use 14442 cells grid, fig. 3.

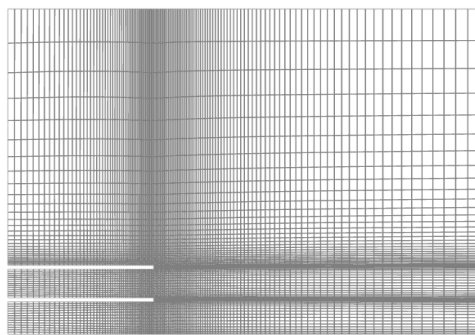


Figure 2. Grid form type used in this study

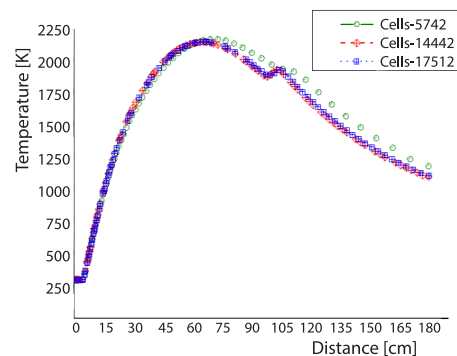


Figure 3. Grid independence test: temperature distribution along the axial direction

The residual of the energy equation should be below 10^{-6} and for all other variables it is set at 10^{-4} to ensure the convergence of the solution. The swirl velocity of components is eliminated in the steady-state CFD study. To investigate various aspects of combustion, the simulation is done in stoichiometric equivalence ratios ($\Phi = 1$).

Second-order discretization scheme is applied to solve all governing equations. The residual of the energy equation should be below 10^{-6} and for all other variables it is set at 10^{-4} to ensure the convergence of the solution. The swirl velocity of components is eliminated in the steady-state CFD study. To investigate various aspects of combustion, the simulation is done in stoichiometric equivalence ratios ($\Phi = 1$).

The instantaneous thermochemical state is described by means of the mixing fraction which represents a single passive scalar when the diffusion coefficients are equal for all chemical species. The mixing fraction is defined [32]:

$$f = \frac{z_i - z_{i,ox}}{z_{i,f} - z_{i,ox}} \quad (15)$$

Results and discussion

Further analysis is conducted on the behavior of the diffusion flame with respect to the composition of the oxidizing current, which we assume to be pure oxygen (100% O_2 , 0% N_2). The analysis involves varying the injection rate of the hydrogen flow and the temperature of the oxygen.

Influence of the air blowing speed

To study the behavior of the temperature in function of different air velocities injection are performed. Hence, the temperature distribution analysis shows that whenever the

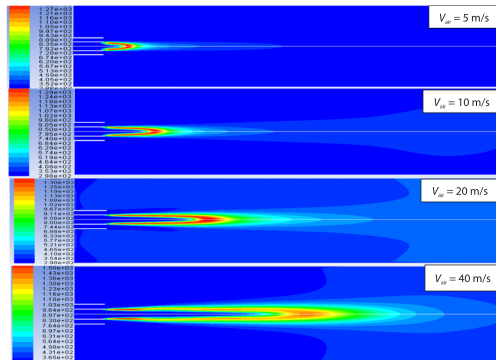


Figure 4. Effect of the air blowing speed on the behavior of the flame

air blowing speed increases, the flame front escapes even more from the injection plane, but the flame no longer takes off from the central injector, fig. 4. It can be seen that the maximum temperature is proportional to the air blowing speed. In this context, a maximum temperature of 1370 K is recorded for $V_{\text{air}} = 5$ m/s. The temperature is rising to 1630K for $V_{\text{air}} = 40$ m/s. This means that the consumption of hydrogen increases, but the maximum temperature shifts backwards, unlike the flame front which escapes forward, forming a kind of flame envelope by enclosing the jet air. This can considerably increase the air-hydrogen contact surface, which promotes better combustion.

Study of the H_2-O_2 flame

We will deal here with the effect of two parameters, namely:

- The hydrogen injection speed.
- The oxygen inlet temperature.

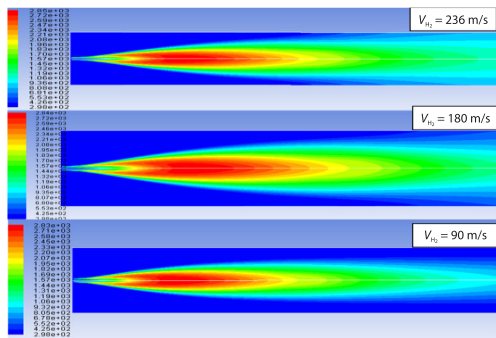


Figure 5. Effect of hydrogen injection speed on the static temperature fields

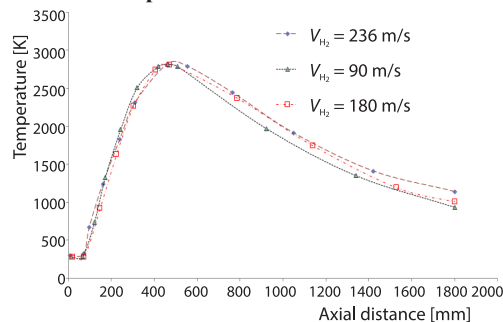


Figure 6. Effect of hydrogen injection speed on the temperature

Effect of hydrogen injection rate

In this case, the rate of introduction of oxygen is 1 m/s and a temperature of 85 K. For hydrogen, the inlet temperature is 287 K, injected at the following respective speeds; 90 m/s, 180 m/s, and 236 m/s. Figure 5 shows that the maximum temperature increases significantly depending on the rate of H_2 injection. For an axial station located at $x = 480$ mm, the maximum values recorded are 2848 K when $V_{H_2} = 236$ m/s and 2839 K for $V_{H_2} = 90$ m/s. Which represents a speed difference about $\Delta V_{H_2} = 146$ m/s. This may indicate that the speed of hydrogen injection does not have a great effect on the value of the maximum temperature to be reach. On the other hand, we can clearly see its influence on the shape of the flame.

Figure 6 illustrates the temperature variations along the direction of the central axis of the combustion chamber. The curve for $V_{H_2} = 236$ m/s is located above that of $V_{H_2} = 90$ m/s, this explains why the flame magnitude for $V_{H_2} = 236$ m/s is slightly large compared to that

of $V_{H_2} = 90$ m/s. The flame core keeps the same shape and illustrates a flame hanging from the nozzle of the injector. The two graphs approximate each other up to $x = 250$ mm which represents a point of intersection.

On the other hand, fig. 7 shows that the slopes of the mass fractions are important, which reveals a rapid disappearance of hydrogen. Indeed, hydrogen has become almost non-existent beyond $x = 600$ mm. We also note that the graph of $V_{H_2} = 90$ m/s is relatively sharp compared to the others, this is explained by the fact that the flame hangs in a place closer to the injectors, than in the case of $V_{H_2} = 236$ m/s where we can note a blowing of the flame which begins to take place.

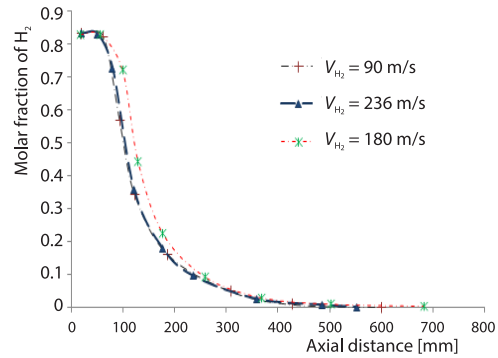


Figure 7. Effect of hydrogen injection speed on the H_2 mass fraction

Effect of oxygen inlet temperature

In this case, the parameters relating to the H_2 flow are maintained ($V_{H_2} = 236$ m/s and $T_{H_2} = 287$ K). The oxygen inlet temperatures are changed as $T_{O_2} = 85$ K, $T_{O_2} = 120$ K, and $T_{O_2} = 300$ K. Figure 8 shows the effect of the oxygen inlet temperature does not seem to be very large on the axial distribution of the static temperature. The visualization of the combustion temperature fields, fig. 9, shows the shapes of the temperatures are the same. However, at the output of the burner, the output temperature for $T_{O_2} = 85$ K is higher than that of $T_{O_2} = 300$ K.

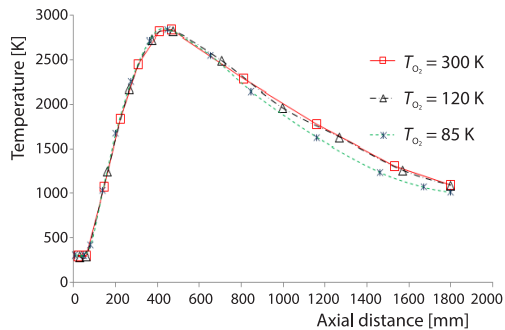


Figure 8. Static temperature distribution on the central axis

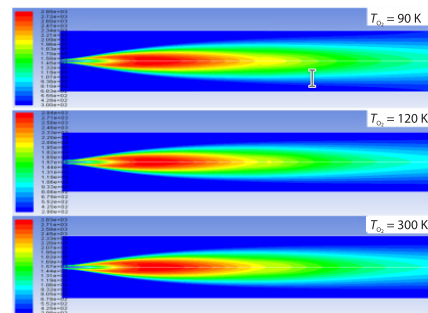


Figure 9. Static temperature fields for different O_2 injection temperatures

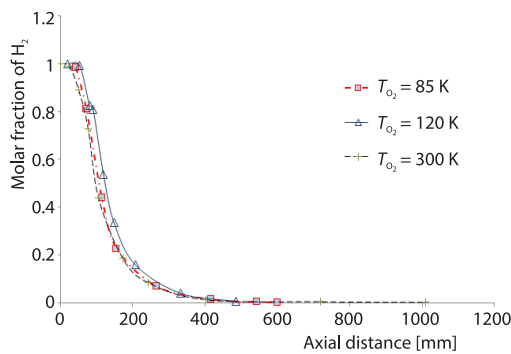


Figure 10. Mass fraction of H_2 for different O_2 inlet temperatures

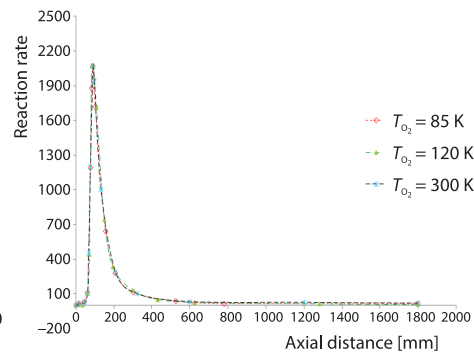


Figure 11. The H_2 reaction rate for different O_2 inlet temperatures

In addition, fig. 10 shows that the slope of hydrogen consumption in the case of combustion with oxygen is greater than the case with air, the oxidation reactions are therefore, faster, although the oxygen injection temperature only slightly influences the consumption of H_2 . This is justified by the variation in the reaction rate plotted as a function of the inlet temperature of the oxygen, fig. 11.

Comparison between hydrogen flames for the case of oxygen and the case of air

In comparison of the case of pure oxygen taken as oxidant (100% O_2 , 0% N_2), fig. 12 shows that the thermal energy released during combustion is greater than for air case. Indeed, the temperature variation on the axis shows the maximum temperature for oxygen (2850 K) is greater than that for air (2130 K) as shown in fig. 13 with a relative rise by 33.80%.

On the other hand, the slope of the plot of oxygen is greater than that of air; which means the reactions in the case of oxygen are faster. This is the reason why the position of the peak of case A is upstream compared to the B case, fig. 13, also, this one requires more time to reach its maximum value, although the maximum temperature for B case is very lower than in A case.

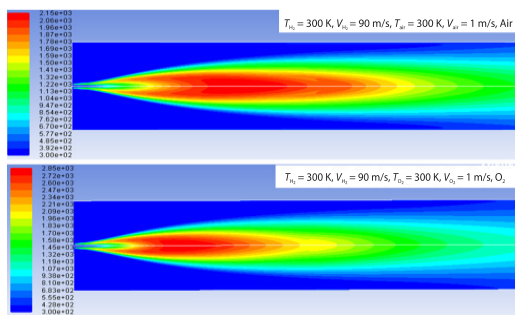


Figure 12. Temperature field for hydrogen combustion difference for air and oxygen case

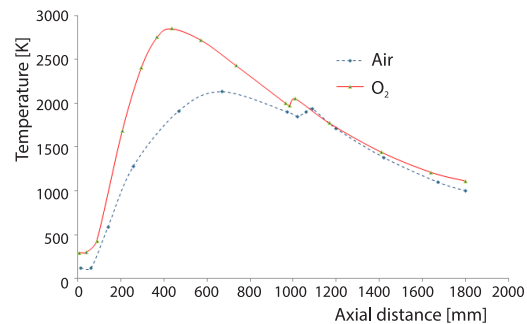


Figure 13. Temperature variation for hydrogen combustion for air and oxygen case

Conclusions

This paper concerns a numerical investigation for the effect of the injection conditions on the structure of the diffusion flame, more specifically, speed and temperature was examined. We are particularly interested in the flame blowing phenomena.

An important remark can be concluded: although nitrogen has an important mass fraction in the air constitutions (78.99% N_2) but hydrogen-air leads to generate non-significant traces of NO_x . On the other hand, it has been observed that increasing the hydrogen injection rate causes the flame to blow away from the injection region, also, the areas with a high temperature gradient are pushed towards the outlet of the combustion chamber away from the injector, which promotes cooling of the nozzle region. The high fuel injection speeds decrease the maximum temperature at the central zone of the tube while they promote an increase in temperatures near the walls of the chamber. The maximum temperature decreases with increasing fuel velocity.

Therefore, the high temperature inlet leads to flame clings to the injection nozzle. Which can represent a dangerous situation by melting the nozzle if the residual time exceeds a certain limit and gives rise to a possibility of flashback if the injection diameter exceeds the

quenching distance of the flame. Also, the flame length decreases when the air inlet temperature and/or the air inlet velocity are increasing so the flame clinging to the injection nozzle. The temperature increases continuously as it advances towards the end of the tube for a low inlet air velocity. That means, for high air speeds, the temperature increases and the length of the flame decreases.

On the other hand, the comparison between the combustion of hydrogen with oxygen with that with air has shown the energy released by the combustion with oxygen is greater for that of the combustion with air. Indeed, by varying the speed of air injection, it has been observed that the flame front moves away from the outlet of the axial injector without leaving it. However, the increasing in the hydrogen injection rate pushes the flame front away from the injection nozzle. The areas of high temperature gradient are pushed out of the tube away from the injector, which helps to cool the nozzle region. The high fuel injection speeds decrease the maximum temperature at the central zone of the tube while promoting an increase in the fuel speed. In addition, it noticed in the two cases previously discussed for combustion with oxygen, the hydrogen appears to be completely consumed upstream of the station $x = 600$ mm.

Nomenclature

$C_{1\epsilon}, C_{2\epsilon}, C_{3\epsilon}$	– constants in k - ϵ model	V	– overall velocity vector, [ms^{-1}]
D_i	– diffusion coefficient of species i	$V_{\text{air}}, V_{\text{gas}}$	– air, gas velocity, [ms^{-1}]
E, h_i	– enthalpy of species i , [J]	x, y	– radial, axial co-ordinates, [mm]
f	– mixture fraction	Y_M	– fluctuating dilatation in compressible turbulence to the overall dissipation rate
G_k	– generation of turbulence kinetic energy due to mean velocity gradients	Greek symbols	
G_b	– generation of turbulence kinetic energy due to buoyancy	ϵ	– dissipation rate of turbulent kinetic energy, [m^2s^{-3}]
J_i	– diffusive flux [$\text{molm}^{-2}\text{s}^{-1}$]	μ	– molecular viscosity
k	– turbulence kinetic energy [m^2s^{-2}]	μ_t	– dynamic turbulence viscosity, [$\text{kgm}^{-1}\text{s}^{-1}$]
n_j	– stoichiometric coefficient for product j	ρ	– mass density
p	– absolute pressure, [Pa]	$\sigma_k, \sigma_\epsilon$	– turbulent Prandtl number for k and ϵ , respectively
Re_g	– Reynolds number for gas	\mathcal{G}	– velocity scale
S_k, S_ϵ	– user-defined source term	$\tilde{\omega}_n, \omega_i$	– density-weighted net rate of production of species n, i [$\text{molm}^3\text{s}^{-1}$]
T	– temperature, [K]		
u_i	– density-weighted cartesian velocity component		

References

- [1] Phebe, A. O., Samuel A. S., A Review of Renewable Energy Sources, Sustainability Issues and Climate Change Mitigation, *Cogent Engineering*, 3 (2016), 1, 1167990
- [2] Koten, H., Hydrogen Effects on the Diesel Engine Performance and Emissions, *International Journal of Hydrogen Energy*, 43 (2018), 22, pp. 10511-10519
- [3] Jose Luis, A., Juan Carlos, B., The Energy Transitionwards Hydrogen Utilization for Green Life and Sustainable Human Development in Patagonia, *International Journal of Hydrogen Energy*, 45 (2020), 47, pp. 25627-25645
- [4] Bakic, V., *et al.*, Technical Analysis of Photovoltaic/Wind Systems with Hydrogen Storage, *Thermal Science*, 16 (2012), 3, pp. 865-875
- [5] Riahi, Z., *et al.*, Numerical Study of Turbulent Normal Diffusion Flame CH₄-air Stabilized by Coaxial Burner, *Thermal Science*, 17 (2013), 4, pp. 1207-1219
- [6] Alrbai, M., *et al.*, Influence of Hydrogen as a Fuel Additive on Combustion and Emissions Characteristics of a Free Piston Engine, *Thermal Science*, 24 (2019), 1, pp. 71-71
- [7] Gupta Ram B., *Hydrogen Fuel: Production, Transport, and Storage*, CRC Press Taylor & Francis Group, Boca Raton, Fla., USA, 2009
- [8] Eichseder H., *et al.*, The Potential of Hydrogen Internal Combustion Engines in a Future Mobility Scenario, SAE Technical paper, 2003-01-2267, 2003

- [9] Lemmon, E. W., *Thermophysical Properties of fluids*, CRC Handbook of Chemistry and Physics, 90th ed. CRC Press, Boca Raton, Fla., USA, Section 6: Fluid Properties, 6.21-6.31, 2009
- [10] Law, C. K., *Combustion Physics*, Cambridge University Press, New York, USA, 2006
- [11] Alliche, M., et al., Extinction Conditions of a Premixed Flame in a Channel, *Combustion and Flame*, 157 (2010), 6, pp.1060-1070
- [12] Syred N., et al., Effect of Inlet and Outlet Configurations on Blow-off and Flashback with Premixed Combustion for Methane and a High Hydrogen Content Fuel in a Generic Swirl Burner, *Applied Energy*, 116 (2014), 1, pp. 288-296
- [13] Karagoz, Y., Koten, H., Effect of Different Levels of Hydrogen + LPG Addition on Emissions and Performance of a Compression Ignition Engine, *Journal of Thermal Engineering*, 5 (2019), 2, Special Issue 9, pp. 58-69
- [14] Karagoz Y., Effect of Hydrogen Addition at Different Levels on Emissions and Performance of a Diesel Engine, *Journal of Thermal Engineering*, 4 (2018), 2, Special Issue 7, pp. 1780-1790
- [15] Alliche, M., et al., Effect of Bluff-Body Shape on Stability of Hydrogen-Air Flame in Narrow Channel, in: *Progress in Renewable Hydrogen and other Sustainable Energy Carriers*, (ed. K. Abdallah), Springer Proceedings in Energy, New York, USA, Chapter 30, 2021, pp. 231-238
- [16] Umyshev, D., et al., Experimental Investigation of Distance between v-Gutters on Flame Stabilization and NO_x Emissions, *Thermal Science*, 23 (2019), 5-B, pp. 2971-2981
- [17] Yang, W., Blasiak, W., Numerical Study of Fuel Temperature Influence on Single Gas Jet Combustion in Highly Preheated and Oxygen Deficient Air, *Energy*, 30 (2005), 2, pp. 385-398
- [18] Alliche, M., Chikh, S., Study of Non-Premixed Turbulent Flame of Hydrogen/Air Downstream Co-Cur-rent Injector, *International Journal of Hydrogen Energy*, 43 (2018), 6, pp. 3577-3585
- [19] Wang, C. J., et al., Predicting Radiative Characteristics of Hydrogen and Hydrogen/Methane Jet Fires Using FireFOAM, *International Journal of Hydrogen Energy*, 39 (2014), 35, pp. 20560-20569
- [20] Dakka, S., Numerical Analysis of Flame Characteristics and Stability for Conical Nozzle Burner, *Journal of Thermal Engineering*, 5 (2019), 5, pp. 422-445
- [21] Shi, L., et al., A Model of Steam Reforming of Iso-Octane: The Effect of Thermal Boundary Conditions on Hydrogen Production and Reactor Temperature, *International Journal of Hydrogen Energy*, 33 (2008), 17, pp. 4577-4585
- [22] Hua, Jingsong, et al., Numerical Simulation of the Combustion of Hydrogen Air Mixture in Micro-Scaled Chambers – Part II: CFD Analysis for a Micro-Combustor, *Chemical Engineering Science*, 60 (2005), 13, pp. 3507-3515
- [23] ***, FLUENT Ansys, Theory Guide. Ansys Inc., 2009
- [24] Khaladi, F. Z., et al., Numerical Simulation of CH₄-H₂-Air Non-Premixed Flame Stabilized by a Bluff Body, *Energy Procedia*, 139 (2017), Dec., pp. 530-536
- [25] Pope, S. B., The PDF Methods for Turbulent Reactive Flows, *Progress in Energy and Combustion Science*, 11 (1985), 2, pp. 119-192
- [26] Obieglo, A., et al., Comparative Study of Modelling a Hydrogen Non-premixed Turbulent Flame, *Combustion and Flame*, 122 (2000), 1-2, pp. 176-194
- [27] Nanduri, J. R., et al., Assessment of RANS-Based Turbulent Combustion Models for Prediction of Emissions from Lean Premixed Combustion of Methane, *Combustion Science and Technology*, 182 (2010), 7, pp. 794-821
- [28] Bilger, R. W., Turbulent Flows with Non-Premixed Reactants, in: *Turbulent Reacting Flows*, Topics in Applied Physics. (Eds.. Libby P. A., Williams F. A.), Springer, Berlin, Heidelberg, 44 (1980), pp. 65-113
- [29] Yakhot, V., Orszag, S. A., Renormalization Group Analysis of Turbulence, I. Basic Theory, *Journal Sci. Comput.*, 1 (1986), Mar., pp. 3-51
- [30] Raman, V., et al., Eulerian Transported Probability Density Function sub-Filter Model for Large-Eddy Simulations of Turbulent Combustion, *Combustion Theory and Modelling*, 10 (2006), 3, pp. 439-458
- [31] ***, <https://www.cerfacs.fr/cantera/mechanisms/hydro.php#boiv>
- [32] Turns, S. R., *An Introduction Combustion: Concepts and Applications*, 3rd ed., Mc Graw Hill, New York, USA, 2012